

HETEROGENEITY IN BULK COMPOSITIONS OF COMPOUND CAIs FROM NWA 3118 AND EFREMOVKA CV3 CHONDRITES. M. A. Ivanova^{1,2*}, A. N. Krot³, N. N. Kononkova¹, and G. J. MacPherson²

¹Vernadsky Institute, Kosygin St. 19, Moscow 119991, Russia. *E-mail: ivanovama@si.edu. ²Department of Mineral Sciences, National Museum of Natural History, Smithsonian Institution, Washington, DC. 20560, USA. ³HIGP/SOEST, University of Hawai'i at Mānoa, Honolulu, HI 96822, USA

Introduction: Calcium-aluminum-rich inclusions (CAIs) are the oldest solar system solids [1,2], and, therefore, provide important constraints on physico-chemical conditions and processes in the protoplanetary disk at the beginning of the solar system formation [3]. Bulk chemical compositions of CAIs in different chondrite groups are characterized by volatility-fractionated trace element patterns, especially the rare earths (REE). One specific pattern, known as “Group II”, is notable for large depletions in the most refractory REE relative to more the more volatile REE [4,5]. This pattern can *only* be explained by fractional condensation from a gaseous reservoir in which the most refractory REEs were removed by prior condensation. However, although CAIs with Group II REE patterns are relatively common, CAIs with the complementary, “ultrarefractory” REE patterns (those having compositions reflecting the earlier condensation episode) are very rare. We recently reported the discovery of two compound CAIs that each contain ultrarefractory (UR) CAIs, #3N from NWA 3118 (CV) and #33E from Efremovka (CV) [6]. Here we report a discovery of third compound CAI, #40E, that hosts an UR CAI within it (#40E-1), from Efremovka. In all three cases the UR nature of these CAIs has been inferred from their mineral chemistry, bulk compositions and comparison with other UR CAIs. REEs patterns, Al-Mg and O isotope systematics will be studied in the future.

Results and discussion: Efremovka CAI #40E is a ~ 1 cm Compact Type A (CTA), and is illustrated in Fig. 1a. The UR-CAI #40E-1 occurs along one margin of #40E and a Ca-Mg-Al-Ti X-ray area map and a BSE image are shown in Figs. 1b and 1c respectively. The CTA #40E is composed of melilite (\AA_{20-30}), spinel, perovskite (~1 wt% V_2O_3), and Zr,Sc-rich pyroxene having 0.31 wt% Zr_2O_3 and 0.61 wt% Sc_2O_3 wt%. The CAI is surrounded by Wark-Lovering (WL) rim layers of spinel, melilite (\AA_{5-10}), and Al,Ti-diopside. The UR CAI consists of melilite (\AA_{5-20}), numerous tiny perovskite grains (~1 wt% V_2O_3 , ~0.86 wt% Zr_2O_3), Zr,Sc-rich pyroxene (Zr_2O_3 and Sc_2O_3 up to 1.2 wt%, V_2O_3 up to 3.2 wt%), and Zr-Sc-rich UNK (a Ca,Al,Ti-oxide phase first described in [7] and experimentally synthesized by [8]). The Zr,Sc-UNK overgrows the Zr-Sc-V-rich pyroxene, and contains 1.9 wt%, Zr_2O_3 and 3.6 wt% Sc_2O_3 . #40E-1 is itself sur-

rounded by the WL rim layers of spinel, melilite (\AA_{5-10}), Al-diopside, and Sc-Zr-rich pyroxene.

The bulk chemical compositions of #40E and #40E-1 are shown in Fig. 2, projected from spinel onto the diagram Al_2O_3 - Ca_2SiO_4 - Mg_2SiO_4 [9]. Also shown are the bulk compositions for the other two compound CAIs noted above, NWA 3118 #3N-24 and Efremovka #33E, along with those of their enclosed UR inclusions. For reference, the general compositional regions of Types A, B, and C CAIs, Fo-bearing Type B (FoB) CAIs, and Al-rich chondrules from CV chondrites are outlined. The composition of 40E is similar to those of typical CTA CAIs, whereas composition of 40E-1 plots outside of and below the field of CTA CAIs in a previously unoccupied region of the diagram. This is due to the unusually high abundance of perovskite, which results in a high Ca/Al ratio. The bulk compositions of five UR CAIs – 3N-24, 33E-1, 40E-1, OSCAR [10], and HIB-11 [11] are shown in a “spider diagram” in Fig. 3, normalized to CI chondrites. All five CAIs are extremely enriched in Zr, Sc, Ti, Ca and V, supporting their ultrarefractory nature.

The distinct mineralogies, oxygen isotopic [6] and bulk chemical compositions of the CAIs forming compound inclusions bearing UR CAIs, indicate that these CAIs formed from mineralogically, chemically, and isotopically distinct precursor materials which may have originated under different (from typical CAIs) physico-chemical conditions, in different regions and/or at different times in the protoplanetary disk. The precursors of the non-UR host CAIs – CTA 40E, FoB 3N and FTA 33E – most likely formed by condensation and melting (40E and 3N) processes commonly involved for the origin of these CAI types [12, 13]. The precursors of UR CAIs – 40E-1, 3N-24 and 33E-1 – composed of very refractory minerals and showing high enrichment in refractory elements compared to typical coarse-grained CAIs, most likely formed by evaporation and/or condensation processes at much higher temperatures than those for the coexisting inclusions 40E, 3N and 33E. More isotope work is needed to distinguish between these options.

References: [1] Amelin Y. et al. 2002. *Science* 297: 1678–1683. [2] Bouvier A. and Wadhwa M. 2010. *Nature Geoscience* 3:637–641. [3] MacPherson G. J. et al. 2005. In *Chondrites and the Protoplanetary Disk*, eds. Krot A. N., Scott E. R. D., Reipurth B., ASP

Conference Series 341:225–251. [4] Boynton W. V. 1975. *Geochim. et Cosmochim. Acta* 39:569–584. [5] Davis A. M. and Grossman L. (1979) *Geochim. et Cosmochim. Acta* 43:611–1632. [6] Ivanova M. A. et al. (2013) *Meteoritics & Planet. Sci.*, 48 (in press). [7] El Goresy A. et al. *Geochim. et Cosmochim. Acta* 48: 2283–2298. [8] Paque J. M. and Stolper E. (1984) *XV LPS*, 631–632. [9] MacPherson G. J. & Huss G. R. 2005. *Geochim. et Cosmochim. Acta* 69: 3099–3127.

[10] Davis A. 1984. *Meteoritics & Planet. Sci.* 19:214. [11] Simon S. B. et al. 1996. *Meteoritics & Planet. Science* 31:106–115. [12] MacPherson G. J. and Grossman L. 1984. *Geochimica et Cosmochimica Acta* 48:29–46. [13] Bullock E. S. et al. 2012. *Meteoritics & Planet. Sci.* 48 (in press).

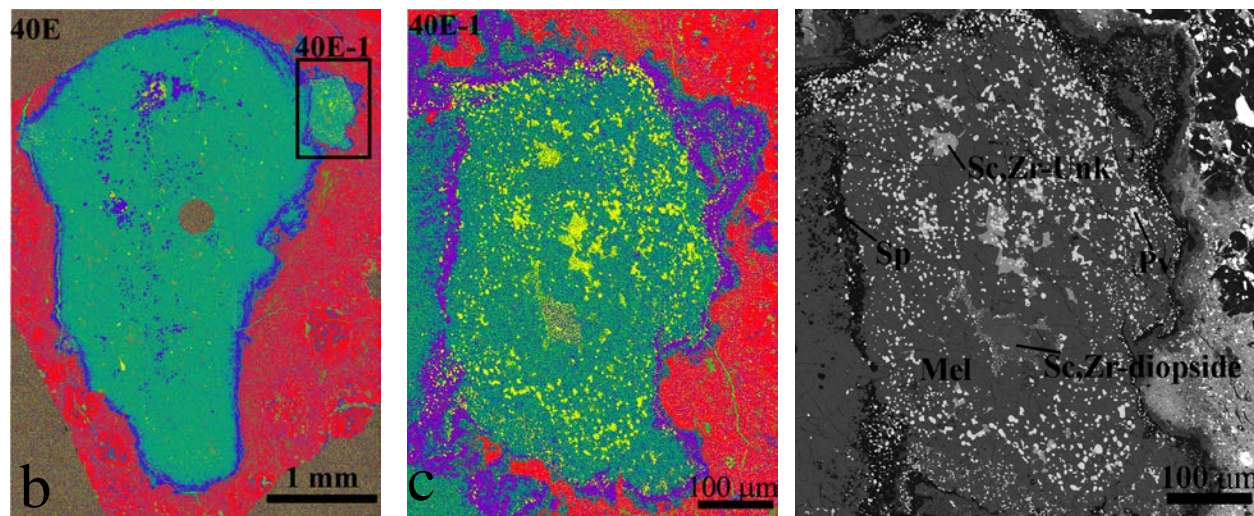


Fig. 1. Combined elemental map in Mg (red), Ca (green), Al (blue), Ti (in yellow) of CTA CAI 40E (a), UR-nodule 40E-1 (b) and BSE image of UR-CAI 40E-1 (c).

Fig. 2. Chemical compositions of CAIs 40E, 40E-1, 3N, 3N-24, 33E, 33E-1.

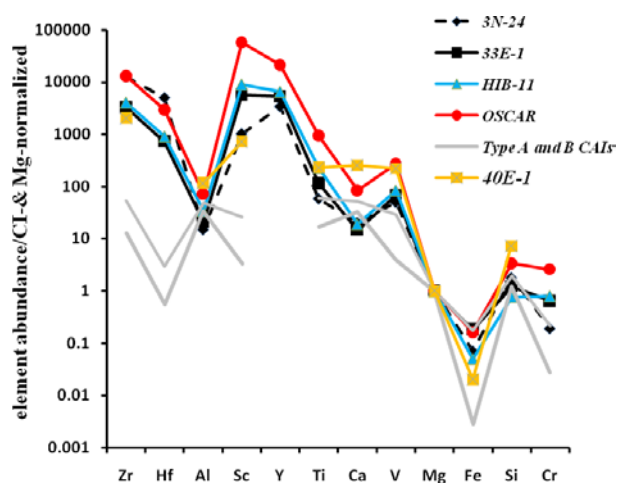
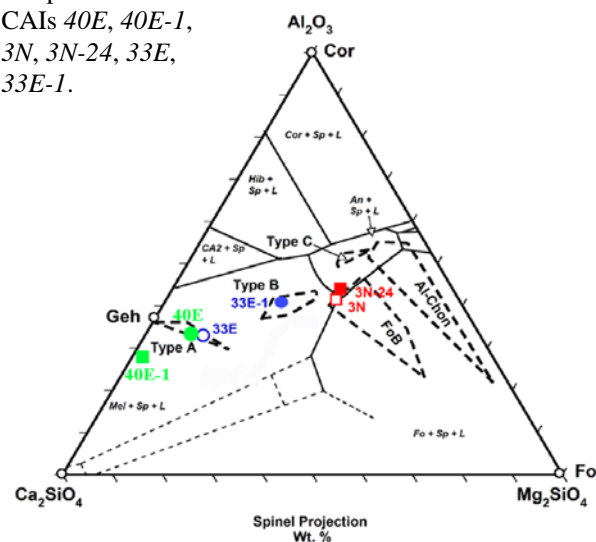


Fig. 3. Chemical compositions of UR CAIs in comparison with Type A and Type B CAIs.